ELSEVIER

Journal of Power Sources 54 (1995) 342–345

JOURNAL OF POWER SOURCES

Origin of the improved cycling capability of sol–gel prepared $Fe_{0.12}V_2O_{5.16}$ compared with V_2O_5

S. Maingot [a], Ph. Deniard [b], N. Baffier [a], J.P. Pereira-Ramos [c], A. Kahn-Harari [a], R. Brec [b], P. Willmann [d]

[a] *ENSCP, Laboratoire Chimie Appliquée Etat Solide, URA 1466, 11 rue Curie, 75005 Paris, France*
[b] *IMN, Laboratoire de Chimie des Solides, 2 rue de la Houssinière, 44072 Nantes, France*
[c] *CNRS, LECSO, UM 28, 2 rue H. Dunant, 94320 Thiais, France*
[d] *CNES, 18 avenue Edouard Belin, Toulouse Cedex, France*

Abstract

A new vanadium iron oxide has been synthesized starting from V_2O_5 xerogel through an exchange reaction. In its Rietveld-determined structure, (FeO_6) apex sharing octahedra link V_2O_5 ribbons and increase the three-dimensional character of the material. This latter point seems to improve the electrochemical behaviour when compared with V_2O_5. Especially, in terms of cycle life, a capacity of 210 Ah/kg is maintained after 40 cycles in the potential window of 3.8–2 V instead of 150 Ah/kg for V_2O_5.

Keywords: Intercalation; Rietveld structure; Iron vanadium oxide; Vanadium oxide

1. Introduction

Starting from molecular precursors to get an oxide network, the sol–gel process allows low-dimensional V_2O_5-based compounds to be prepared. In general, $M_xV_2O_5$ bronzes with a monoclinic symmetry are obtained (M = Na, Li, K, Ag) [1]. In these compounds, vanadium is reduced accordingly by the inserted metal. These bronzes reversibly intercalate lithium. For instance, $Na_{0.33}V_2O_5$ bronze presents a good behaviour as a cathode material in a secondary non-aqueous lithium battery [2].

The synthesis of $Fe_{0.12}V_2O_{5.16}$ was performed as reported in Ref. [3]. The formulation $Fe_{0.12}^{3+}V_{1.96}^{5+}V_{0.04}^{4+}O_{5.16}^{2-}$ is in complete agreement with the occurrence of 2% of V^{4+} already present in the xerogel. This V^{4+} content, determined by potentiometric measurement through V^{4+} oxidation by potassium permanganate, is consistent with the fact that this compound is not a bronze but a double oxide.

2. X-ray sample preparation

The sample was prepared by ultrasonic grinding in an ethanol medium to avoid preferential orientation, always encountered in such a material. The X-ray diagram was recorded on an INEL CPS 120 curve detector in a Debye–Scherrer geometry on 20 μm particles filling a 0.1 mm Lindemann capillary. This technique allows the use of a tiny amount of powder available after sonics and prevents greatly from preferential orientation [4]. The structure refinement was carried out by the Rietveld refinement code GSAS [5].

3. Results

3.1. Structure refinements

The cell parameters of $Fe_{0.12}V_2O_{5.16}$ yields values not very different from those of V_2O_5. A slight decrease of the *c*-parameter and increase in the *a*-parameter are observed ($a = 11.5415(7)$, $b = 3.5642(2)$ and $c = 4.3596(3)$ Å as compared with the V_2O_5 ones ($a = 11.5119(8)$, $b = 3.5646(2)$ and $c = 4.3748(3)$ Å). For this reason, the calculations were started assuming that both vanadium and oxygen atoms were located in the same positions of the *Pmmn* space group as in V_2O_5. A successful refinement was obtained with the V_2O_5 framework and with iron atoms located in 2*a* sites, between four oxygen atoms of the V_2O_5 slab with an

SSDI 0378-7753(94)02097-M

occupation ratio refined to $\tau = 0.110(8)$. The calculation used 19 variables and 1799 observations with the following confidence factors: $R_{wp} = 0.038$, $R_p = 0.030$ and $R_{exp} = 0.013$, the light oxygen atoms having their atomic displacement parameter (ADP) fixed for stability reasons. Atomic positions and cell parameters are given in Table 1. The iron concentration fits very well with the chemical analysis. However, Fe^{3+} ions are not stable in square coordination and since the d_{Fe-O} distances match that of the Fe^{3+} in oxygen octahedral surrounding, two additional oxygen atoms have to be localized above and below the Fe ions, along the *c*-axis, in order to achieve an octahedral oxygen environment at the Fe–O distance corresponding to the average refined ones (2.180 Å). (Due to very weak contribution to the overall diffraction diagram, these two extra atoms positions were not introduced. Indeed, they could not be detected on the Fourier map difference.)

The structure of $Fe_{0.12}V_2O_{5.16}$ plotted with the Molview program [6] is given in Fig. 1. Vanadium and iron environments are given in Table 2.

The V(1)–O(2) distance (1.37 Å) is very short as compared with the same one found in V_2O_5 (1.6 Å), probably in relation with the presence of iron atoms in the vicinity of vanadium. In fact, such short distances are encountered in the literature for $Pb_3V_2O_8$ [7] and NaV_6O_{15} [8] for example, with V–O shortest distances, respectively equal to 1.435 and 1.388 Å.

3.2. Structural discussion

According to their stoichiometry, the Fe ions do not fill all the available 2*a* sites of the structure. The structural arrangement of FeO_6 octahedra is not known exactly but some extreme conditions can be rejected: (i) the charge balance implies than an infinite chain of apex sharing FeO_6 octahedra, along the *c*-axis, cannot be considered (in addition, it would imply a Fe/O ratio equal to one, leading to a formulation $Fe_{0.12}V_2O_{5.12}$), and (ii) isolated FeO_6 octahedra cannot exist because, in that case an $Fe_{0.12}V_2O_{5.24}$ formulation would be found, too far from the experimental one ($Fe_{0.12}V_2O_{5.16}$).

Table 1
Atomic positions in $Fe_{0.12}V_2O_{5.16}$. Atomic displacement parameters were fixed for oxygen atoms; (O*: additional oxygen not introduced into the calculation completing the Fe^{3+} octahedral environment) *

Atom	*x*	*y*	*z*	Occupation	$100 \times U_{iso}$
V(1)	0.3994(6)	1/4	0.071(2)	1	4.2(4)
O(2)	0.388(1)	1/4	0.384(4)	1	1
O(3)	0.562(1)	1/4	0.967(5)	1	1
O(4)	1/4	1/4	0.004(7)	1	1
Fe(5)	3/4	1/4	0.03(2)	0.110(8)	1
O*	3/4	1/4	−0.468		

* Space group: *Pmmn*; $a = 11.5415(7)$, $b = 3.5642(2)$, and $c = 4.3596(3)$ Å.

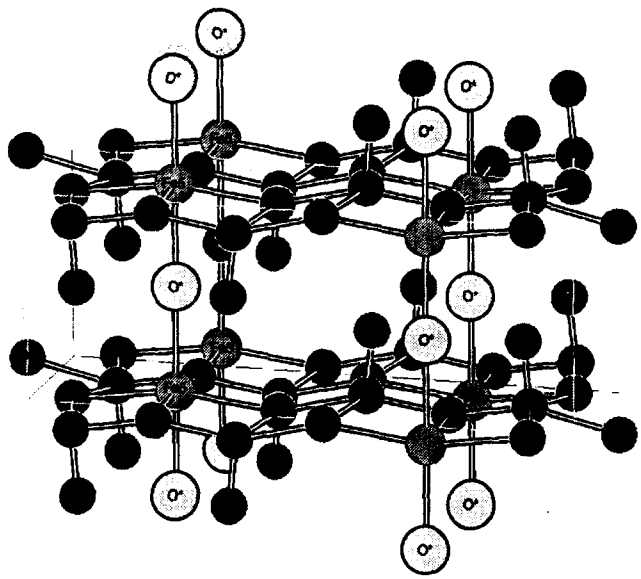

Fig. 1. Perspective view of $Fe_{0.12}V_2O_{5.16}$ structure. Fe^{3+} (●) is located within the ribbons of V_2O_5. Extra oxygen atoms (O*) complete the iron octahedral environment. This is an average description: not all Fe sites are occupied.

Table 2
Vanadium and iron environment distances and angles; (O*: unrefined additional oxygen completing the Fe^{3+} octahedral environment.)

Interatomic distances (Å)		Angles (°)	
V(1)–V(1)	2.991(11)×2	O(2)–V(1)–O(3)	96.4(8)
V(1)–O(2)	1.369(17)	O(2)–V(1)–O(3)	109.0(13)
V(1)–O(3)	1.844(5)×2	O(2)–V(1)–O(3)	96.4(8)
V(1)–O(3)	1.932(15)	O(2)–V(1)–O(4)	94.2(14)
V(1)–O(4)	1.749(9)	O(3)–V(1)–O(3)	75.2(6)
V(1)–Fe(5)	2.520(16)×2	O(3)–V(1)–O(3)	150.3(11)
		O(3)–V(1)–O(4)	102.8(7)
		O(3)–V(1)–O(3)	75.2(6)
		O(3)–V(1)–O(4)	156.8(12)
		O(3)–V(1)–O(4)	102.8(7)
Fe(5)–V(1)	2.520(16)×4	O(3)–Fe(5)–O(4)	89.3(7)
Fe(5)–O(3)	2.186(26)×2	O(3)–Fe(5)–O(3)	165.1(17)
Fe(5)–O(4)	1789(9)×2	O(3)–Fe(5)–O*	97.44
Fe(5)–O*	2.180×2	O(3)–Fe(5)–O*	82.55
		O(4)–Fe(5)–O*	84.97
		O(4)–Fe(5)–O*	95.03
		O(4)–Fe(5)–O(4)	170.0(7)
		O*–Fe(5)–O*	180.0

Additional information is given in the X-ray powder diagram by the presence of a small peak around 12.41° 2θ. This position corresponds exactly to the 010 line with a *b*-doubled parameter superstructure. A preliminary Mössbauer study has given some information on the FeO_6 chains along the *c*-axis. This study confirms the oxidation state 3 for Fe ions and the differently distorted octahedral environments observed confirm the hypothesis of finite FeO_6 chains. This increases the three-dimensional character of the compound by linking the V_2O_5-like ribbons. This last point seems to be at

the origin of the improved electrochemical behavior of $Fe_{0.12}V_2O_{5.16}$ as compared with V_2O_5.

3.3. Electrochemical behaviour

A stainless-steel grid of 1 cm^2, on which the material mixed with graphite (90 wt.%) was pressed, composed the positive electrode, whereas the negative electrode consisted in a lithium foil. The electrolyte was double-distilled propylene carbonate and anhydrous lithium perchlorate dried under vacuum at 200 °C for 12 h. The electrolyte preparation (1 M $LiClO_4$) and the cell assembling were done under a purified argon atmosphere.

During lithium intercalation under galvanostatic soft conditions ($i = 20$ μA, $C/40$), $Fe_{0.12}V_2O_{5.16}$ presents a four-step reduction in the 3.5–1.8 V potential range, with 3 lithium ions intercalated per formula (Fig. 2) [9]. This first discharge corresponds to a 440 Ah/kg capacity. A coulombmetric titration curve for the first two steps of lithium intercalation is compared with V_2O_5 in Fig. 3. Although a similar shape is found for both compounds, a lower lithium uptake is reached for $Fe_{0.12}V_2O_{5.16}$. For a cutoff voltage of 3 V, about 0.80 lithium ions are accommodated in this compound versus ≈ 0.95 in V_2O_5. This may be correlated to the additional oxygen sites normally available for lithium intercalation.

The influence of the current density (Fig. 4) shows that $Fe_{0.12}V_2O_{5.16}$, unlike V_2O_5, maintains a remarkable capacity, even at a higher current density. One finds 2.7 F/mol for a current density of 100 μA/cm^2.

After the first discharge, cycle-life tests have been undertaken [10]. A $C/4$ cycling rate was imposed by CNES (Centre national d'études spatiales), as these batteries are designed to be used as power sources in satellites. In Fig. 5, a mass capacity higher than 250

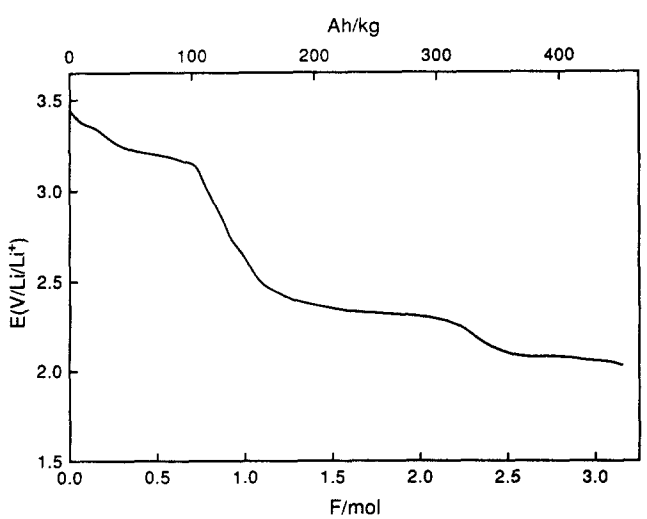

Fig. 2. $Fe_{0.12}V_2O_{5.16}$ galvanostatic discharge curve at $C/40$ rate using 1 M $LiClO_4$ in propylene carbonate as solvent.

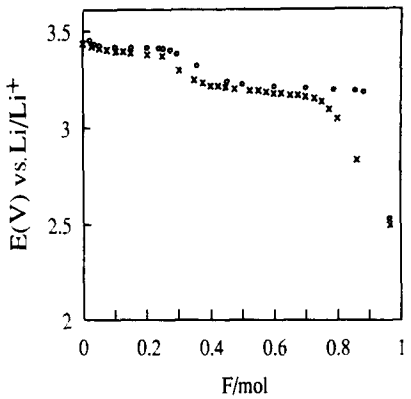

Fig. 3. Comparison of the first two steps of lithium intercalation in (×) $Fe_{0.12}V_2O_{5.16}$ and (○) V_2O_5 at 20 °C.

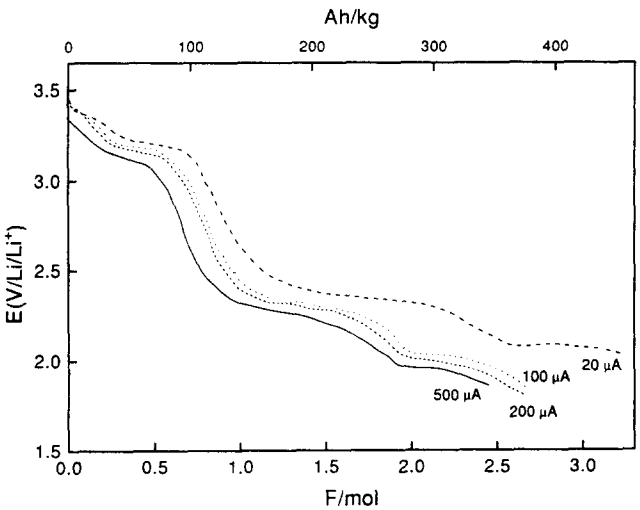

Fig. 4. $Fe_{0.12}V_2O_{5.16}$ chronopotentiograms under different current densities.

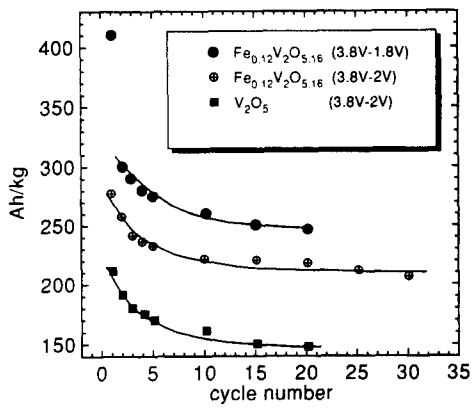

Fig. 5. Capacity evolution of $Fe_{0.12}V_2O_{5.16}$ compared with V_2O_5 in a potential range from 3.8 to 2 V and of $Fe_{0.12}V_2O_{5.16}$ with a potential down to 1.8 V.

Ah/kg is maintained after 20 cycles in a potential window implying all the oxidation/reduction plateaus. Down to 2 V, the capacity stabilizes to 210 Ah/kg for 40 cycles when only a 145 Ah/kg capacity is recovered at 20 cycles for V_2O_5. The loss of capacity at 20 cycles is

20% for $Fe_{0.12}V_2O_{5.16}$ whereas it corresponds to 30% for V_2O_5 for the same cycle number.

4. Discussion and conclusions

The occurrence of $[FeO_6]$ octahedra chains in $Fe_{0.12}V_2O_{5.16}$ induces interesting features, especially in terms of cycle life at a high discharge rate ($C/4$). These iron files increase the three-dimensional character of the compound, creating a link between V_2O_5-like ribbons. These chains which are finite, along the c-axis, strengthen the cohesion between the layers, maintaining the structure through cycling. Further Mössbauer measurements have to be done to evaluate the lengths of the iron chains but an order between these chains, corresponding to a b-cell parameter doubling, seems to be unquestionable, referring to the small diffraction peak observed in the X-ray powder diagram.

References

[1] L. Znaidi, N. Baffier and M. Huber, *Mater. Res. Bull., 24* (1989) 1501.
[2] J.P. Pereira-Ramos, L. Znaidi, N. Baffier and R. Messina, *Solid State Ionics, 28–30* (1988) 886.
[3] N. Baffier, L. Znaidi and M. Huber, *Mater. Res. Bull., 25* (1990) 705.
[4] S. Maingot, Ph. Deniard, N. Baffier, J.P. Pereira-Ramos, A. Kahn-Harari and R. Brec, in J. Rouxel, M. Tournoux and R. Brec (eds.), *Soft Chemistry Routes of New Materials,* Trans. Technical Publication, Aedermannsdorf, Switzerland, 1994.
[5] A.C. Larson and R.B. von Dreele, *LANSCE MS-H805 Los Alamos National Laboratory,* Los Alamos, NM 87545, USA.
[6] J.M. Cense, *Thesis*, Ecole Nationale Supérieure de Chimie de Paris, France.
[7] P. Garnier, G. Galvarin, J.F. Berar and D. Weigel, *Mater. Res. Bull., 19* (1984) 407.
[8] T.N. Khamaganova and V.K. Trunov, *Russ. J. Inorg. Chem., 34* (1989) 164.
[9] S. Maingot, R. Baddour, J.P. Pereira-Ramos, N. Baffier and P. Willmann, *J. Electrochem. Soc., 140* (1993) 158.
[10] J.P. Pereira-Ramos, R. Baddour, N. Baffier and P. Willmann, *Fr. Patent No. 9 115 495.*